

# Some Studies on Autogenous Automated GTA Welding of 2205 Grade Duplex Stainless Steel

<sup>1</sup>S. Sankarapandian and <sup>2</sup>K. P. Padmanaban

## ABSTRACT

Autogenous Automated Gas Tungsten Arc Welding (AA-GTAW) is a familiar and vastly employed welding method to weld 2205 grade Duplex stainless steel (DSS). In this study the notable course criterions of welding mainstream like welding speed (S), welding current (I) and arc length (L). With Response Surface Methodology (RSM), the effective use of these criterions are brought on the responses of bead geometry such as Bead Width (BW), Depth of Penetration (DoP) and Weld Area (WA) are determined. The input process parameters are varied at three levels of full factorial design hence 27 experimental trials were conducted. Bead on plate (BoP) welding trials were conducted using DSS sheet of 2 mm thickness. Simultaneous effects of welding parameters on various responses were obtained by applying RSM through three separate second order polynomial quadratic equations. ANOVA analysis helps to verify the adequacy and significance of the improved model. Moreover, optimized values for the parameters employed in the welding process parameters to attain the expected geometry of weld bead that influences that the mechanical properties of the joint is found. Finally, the optimized parameters are validated by conducting confirmation experiments.

**Keywords:** Autogenous Automated Gas Tungsten Arc Welding, Duplex Stainless Steel, Weld bead geometry, Response surface methodology.

## 1. INTRODUCTION

Most of the industrial applications such as oil and gas, power, desalination plants, oceanic areas, paper industry, and pipes in chemical tankers, bridges, food and beverage industries, apparatus for structural design, storage tanks run through DSS of grade 2205. It possesses superior corrosion resistance, strength, good weldability, stress corrosion cracking, good wear, abrasive resistance, and low thermal expansion and fatigue properties. The quality of DSS is determined by the balanced fractions of FCC austenite ( $\gamma$ ) and BCC ferrite ( $\delta$ ). These two states having various similarities for blending elements in DSS [1]. The optimum property of the DSS depends on the  $\gamma$  &  $\delta$  proportions present in the microstructure. To obtain this state balance in base metals, by suitable fusion of configuration and solution heat treatment [2]. In welding, it is very critical to maintain the phase balance of DSS. Desired ferrite content in the weld joint 30-55% for better performance of DSS [3]. Ferrite content less than 25 % in the welded joint lead to reduction in strength and risk of the stress corrosion cracking, more than 75% ferrite content in the welded joint reduced corrosion resistance and impact toughness. The 2205 DSS contents of high chromium and molybdenum provides high protection to crater and fissure deterioration. Also possesses high resistant to chloride stress corrosion cracking leads to superior strength, toughness and good weldability [4].

<sup>1</sup> Assistant Professor, Department of Mechanical Engineering, Alagappa chettiar college of Engg & Tech., Karaikudi 630 003, Tamilnadu, India, E-mail: [sankarapandian1027@gmail.com](mailto:sankarapandian1027@gmail.com)

<sup>2</sup> Principal, Kurinji college of Engg & Tech, Manapparai 621 307, Tamilnadu, India

Thickness less than 5mm plates or sheets are weld joined by melting of edges. The weld joint developed by melting and faying surfaces and subsequently solidification only (without using any filler metal) is called autogenous weld. Thus, the composition in the autogenous weld metal corresponds to the parent metal only. Geometry of the weld bead defines the quality of TIG welding and mechanical property of the weld. Hence selecting appropriate welding parameters is necessary for obtaining optimal weld pool geometry [5]. TIG welding produces high quality welds on thin materials. Gao et al reported that for welding thin sheets, the edge arrangements and filler metals are not needed. In Gas Tungsten Arc Welding (GTAW), the torch head is surrounded by shielding medium which covers the instantaneous molten pool. Due to substantial generation of heat generated in the welding process, the welding material becomes distorted and coarse grains are formed in it. This is one of the demerits of the GTAW process [6]. Cemal Meran also ascertains that welding current, one of the process parameter of GTAW, affects the weld geometry. He also states that the size and shape of the weld pool is controlled by speed and arc length [7]. Magudeeswaran et al discussed that the influence of electrode gap is the predominant factor of ATIG welding to affect the aspect ratio by Taguchi method of DSS joints. Also for aspect ratio of 1.24 for the joints, ferrite number is in good percentage and no solidification cracking occurred [8]. Kiaee et al reported that desired mechanical properties of the weld can be obtained by controlling various welding variables such as current, travelling speed and rate of shielding gas flow. From this it is also ascertained that welding speed impacts the tensile strength and hardness of material in GTAW of A516-Gr 70 carbon steel [9]. Juang et al discussed that the choice of process parameters for TIG welding are optimized by Taguchi method and concludes that smaller the better quality characteristics i.e. the front width, front height, back width and back height makes the optimal weld pool in stainless steel [10]. Karpagaraj et al in their AA-TIG welding process have optimized current and torch speed input parameters while conducting bead on plate trials which resulted in full penetration of cp titanium thin sheets [11]. Korra et al revealed that in performing of A-TIG welding process, three parameters namely current, torch speed and arc gap have positive impact on the profile of the weld bead of DSS. Further it was found that RSM is used to optimize the responses of the above experiment [12].

Design of Experiments (DOE) technique is used for optimization of process variables. Based on the survey of literature it is found that only a handful of research work is carried out on AA-GTA welding experiment involving thin sheets of Duplex Stainless Steel. Hence, an attempt is endeavour contrived in this proposed work to develop the process parameters by using RSM for modeling, analysis and optimization on AA-GTA welding of thin duplex stainless steel sheet of grade 2205.

## 2. EXPERIMENTAL WORK

2205 DSS sheets of 2 mm thick sheets are utilized for the present analysis. The composition of chemical ingredients present in 2205 DSS is listed in Table 1. The welding of 2205 DSS is done using AA- GTA welding machine (FRONIUS MAGIC WAVE 400) as indicated in Fig. 1.

**Table 1**  
**Chemical composition (wt %) of 2205 DSS alloy**

<i>Cr</i>	<i>Mo</i>	<i>Ni</i>	<i>N</i>	<i>C</i>	<i>Mn</i>	<i>Si</i>	<i>P</i>	<i>S</i>	<i>V</i>	<i>Ti</i>	<i>Co</i>	<i>Fe</i>
23.0	3.5	6.5	0.20	0.03	2	1	0.03	0.02	0.06	0.004	0.01	Balance

Numerical control unit helps to control the welding speed. Depending on the weld experience and literature, it is concluded that among the doable AA-GTA welding process input parameters like that of welding current (I) in amperes, arc length (L) in mm and welding speed (S) in mm/second are the causes that decide the heat that is given as input for the work piece. Therefore, it has been decided that bead on plate trials will be conducted by changing the welding speed (S), welding current (I) and arc length (L) as shown in Table 2.



Figure 1: Image showing GTA Welding Experimental Setup

**Table 2**  
Selection of process parameters and levels

<i>Parameter</i>	<i>Level 1</i>	<i>Level 2</i>	<i>Level 3</i>
Welding Current (I) in Amperes	60	80	100
Welding Speed (S) in mm/sec	250	300	350
Arc Length (L) in mm	2	3	4

A three-level speculative design with the welding speed, welding current and arc length has been chosen in a Full-Factorial scheme ( $3^3$  Design refers to the three autonomous variables that has three levels each). To produce full penetration it is planned to conduct the bead on plate (BoP) trails by changing the input process variables which has a considerable influence on geometry of the weld bead. The electrode diameter of 2.4mm is kept constant for all the experimental trials. Prior to conducting the BoP trials, wire brush and acetone were used to unblemish the thin sheets of 2205 DSS. Through the proportions above, twenty seven bead on plate trials are conducted in 2205 DSS sheets for the various combinations of input parameters. Based on the trials conducted, 2205 DSS samples were made ready using wire Electrical Discharge Machine in the cross wise direction of the weld. Then it was mounted with Bakelite. Various rating of emery sheets glisten all specimens. A solution comprising of 36% Hydrochloric acid, 1% Hydrogen Fluoride, 0.8gm potassium Meta bisulphate and 63% of water is availed as etchant medium to bring to light the profile of weld bead. The graphic representation of the geometry of weld bead is represented in Fig. 2.

Macrographs are acquired with a Weld Expert System (Struers, Austria) that consists of an enlarged variation between 20X – 240X. Some selected samples microstructures are shown in Figs.3 (a) – (d). The responses of depth of penetration (DoP), bead width (BW) and weld area (WA) are shown in Figs.4 (a)-(c) for various experimental trials.

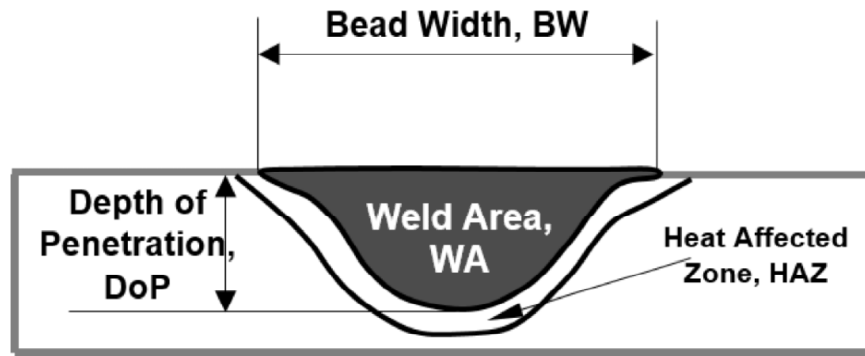


Figure 2: Graphic representation of weld bead geometry

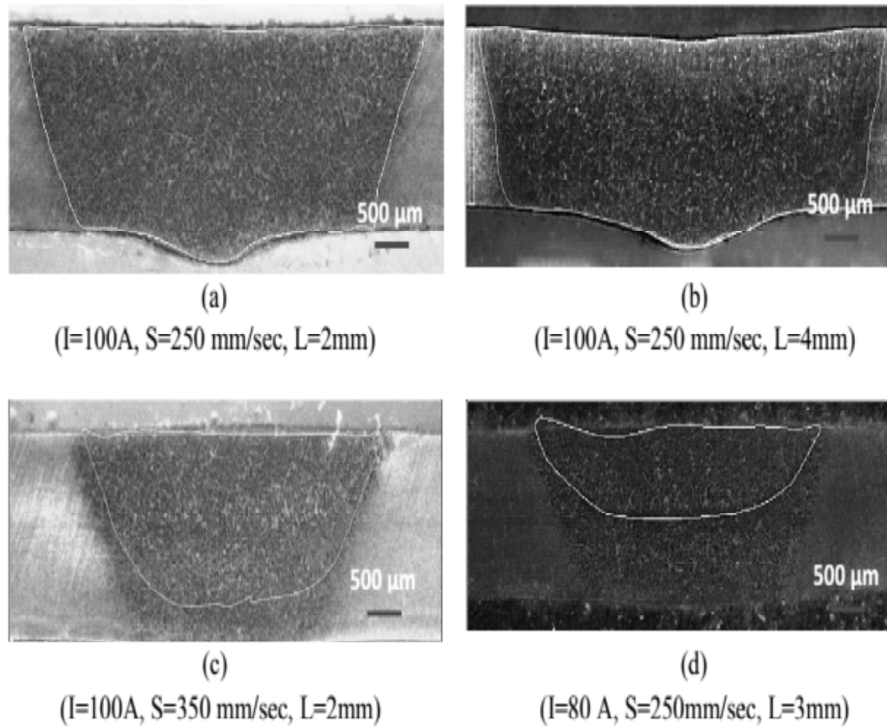
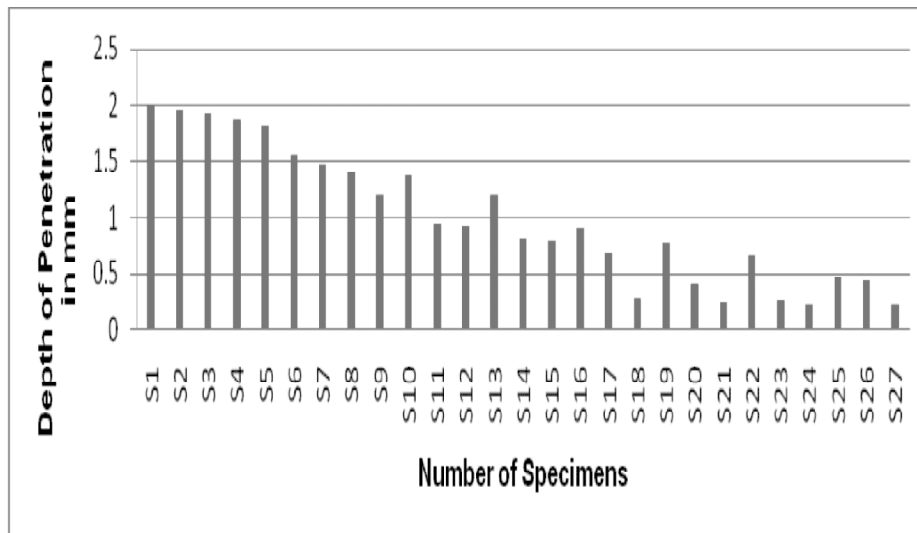
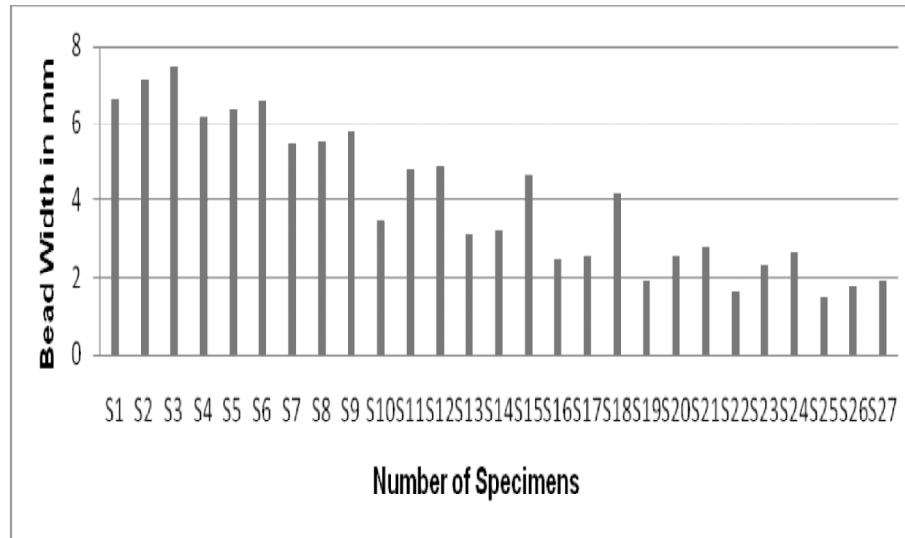


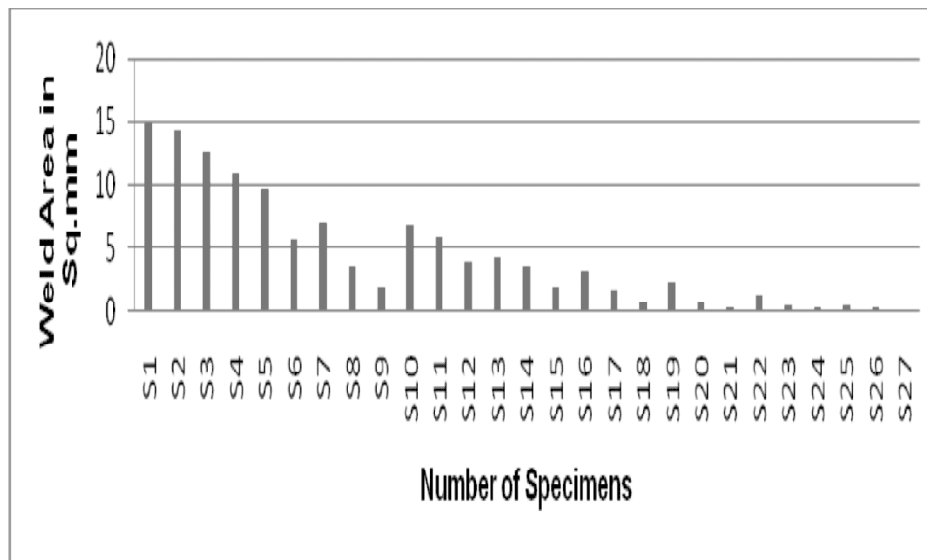
Figure 3: (a) – (d) Macrographs of Bead on plate trials for different input process parameters



(a)



(b)



(c)

Figure 4: (a)-(c) Response of (a) DoP, (b) BW and (c) WA

### 3. RESPONSE SURFACE METHODOLOGY

This statistical technique helps to model, optimize and to analyse the problems. Numerous variables were influence the response of interest. Its ultimate aim is to make the results best [13]. In this RSM technique the cause and effect relationship between input control variables and true mean responses should be determined and represented. It influences the responses as a two dimensional or three dimensional hyper surface and also establishes the association between the input variables of the welding process and the essential reactions [14]. Finally the aim is optimizing of response through evaluation of the codes of input process variables used in welding process. The optimized value can be minimum or maximum subject to a particular set of variables.

#### 3.1. Developing mathematical model

Statistics pertaining to the parameter for the AA-TIG welding of 2205 DSS was analyzed using the Design Expert V9 software. RSM helps to improve the mathematical relationships between the welding variables

and the responses. It is developed to determine the geometry of the weld bead with optimum desired values. The application of RSM technique is done wherein the surface of analyzed independent variables the mathematical models are fitted. After which a second order polynomial equation is generated to represent the response surface that was fitted to the data [15]. The best fit model is obtained and sequential F test and ANOVA are carried out.

### 3.1.1. Mathematical modeling for Depth of Penetration (DoP)

To estimate the significance of the model, ANOVA is performed and it is 95% of the significance level. If the  $p$  value is below 0.05, the model is considered as noteworthy. ANOVA analysis was conducted to determine if there is significant effect on weld bead geometry due to the interaction of variables taken into consideration in the AA-GTA welding process. Further it is also used to find if the model developed is significant. An ANOVA analysis depicting the depth of penetration (DoP) is pictured in Table 3. The related  $p$  value is less than 0.05 for the model (95% confidence level) indicates that the model terms are numerically important. Design expert software was used to create the regression model for depth of penetration as significant. Adjacent  $R^2$  close to 1, which shows the model adequate. The R-squared value and the predicted R-squared value such as 0.9766 and 0.9378 are in reasonable agreement with adjusted R-squared that is 0.9642 as shown in Table 4. In this case, welding speed (S), welding current (I), arc length (L), the interaction factor IS and the quadratic term welding current ( $I^2$ ) are significant model terms. The mathematical model finally derived based on the actual factors for predicting the depth of penetration (DoP) as shown below:

$$\begin{aligned} \text{Depth of Penetration (DoP)} = & -1.059539 - 0.006133 I + 0.017445 S - 0.571533 L - 0.000125 \\ & I*S + 0.002535 I*L - 0.000151 S*L + 0.000426 I^2 - 0.0000181 S^2 + 0.037683 L^2 \end{aligned} \quad (1)$$

**Table 3**  
ANOVA analysis for DoP

Source	Sum of Squares	df	Mean Square	F Value	p-value Prob > F	
Model	9.1900	9	1.0211	78.8414	4.40425E-12	significant
I-Welding Current	7.4667	1	7.4667	576.5099	1.48132E-14	
S-Welding Speed	0.6737	1	0.6737	52.0164	1.45297E-06	
L-Arc Length	0.6357	1	0.6356	49.0776	2.11667E-06	
IS	0.1872	1	0.1872	14.4578	0.0014	
IL	0.0308	1	0.0308	2.3809	0.1412	
SL	0.0007	1	0.0007	0.0527	0.8211	
$I^2$	0.1745	1	0.1745	13.4699	0.0019	
$S^2$	0.0123	1	0.0123	0.9500	0.3434	
$L^2$	0.0085	1	0.0085	0.6578	0.4285	
Residual	0.2201	17	0.0129			
Cor Total	9.4102	26				

**Table 4**  
R-Squared value for DoP

Std. Dev.	0.1138	R-Squared	0.9766
Mean	0.9890	Adj R-Squared	0.9642
C.V. %	11.5066	Pred R-Squared	0.9378
PRESS	0.5848	Adeq Precision	29.6116

### 3.1.2. Mathematical modeling for bead width (BW)

Table 5 reveals the bead width ANOVA analysis. The model developed for bead width (BW) was in quadratic form and it is significant. As per the analysis the values for R-squared value and Predicted R-squared value are 0.9777 and 0.9478 respectively. It is in terms of reasonable agreement with adjusted R-squared value that is 0.9659 shown in table 6. In this case, also welding speed (S), welding current (I), arc length (L), the interaction factor IS and the quadratic term welding current (I<sup>2</sup>) are significant model terms. The mathematical model finally derived based on the actual factors for predicting the bead width (BW) as shown below:

$$\text{Bead Width (BW)} = -1.350378 - 0.040803 I + 0.015725 S + 0.757033 L - 0.000193 I*S - 0.002975 I*L - 0.000983 S*L + 0.001334 I^2 - 0.0000151 S^2 + 0.0417 L^2 \quad (2)$$

**Table 5**  
ANOVA analysis for BW

Source	Sum of Squares	df	Mean Square	F Value	p-value	Prob > F
Model	92.98	9	10.3311	82.9418	2.9E-12	significant
I-Welding Current	80.4462	1	80.4462	645.8503	5.78E-15	
S-Welding Speed	6.2341	1	6.2341	50.0496	1.87E-06	
L-Arc Length	4.0501	1	4.0501	32.5228	2.59E-05	
IS	0.4493	1	0.4493	3.6069	0.0746	
IL	0.0425	1	0.0425	0.3412	0.5668	
SL	0.0289	1	0.0289	0.2326	0.6358	
I <sup>2</sup>	1.7090	1	1.7090	13.7206	0.0018	
S <sup>2</sup>	0.0086	1	0.0085	0.0689	0.7963	
L <sup>2</sup>	0.0104	1	0.0104	0.0838	0.7758	
Residual	2.1175	17	0.1245			
Cor Total	95.0975	26				

**Table 6**  
R-Squared value for BW

Std. Dev.	0.3529	R-Squared	0.9777
Mean	4.0444	Adj R-Squared	0.9659
C.V. %	8.7263	Pred R-Squared	0.9478
PRESS	4.9587	Adeq Precision	29.5826

### 3.1.3. Mathematical model for weld area (WA)

ANOVA analysis was conducted for the weld area and it is depicted in Table 7. The model developed for weld area (WA) was in quadratic form and it is significant. The estimated value for R-squared and Predicted R-squared consists of 0.9684 and 0.9103 respectively. It is in reasonable agreement with adjusted R-squared estimation that is 0.9517 shown in table 8. In this case, welding speed (S), arc length (L), welding current (I), the interaction factor IS and the quadratic term welding current (I<sup>2</sup>) are significant model terms. The mathematical model finally derived based on the actual factors for predicting the weld area (WA) as shown below:

$$\text{Weld Area (WA)} = -29.139305 + 0.481552 I + 0.071363 S + 2.358378 L - 0.002192 I*S - 0.037828 I*L - 0.000431 S*L + 0.003091 I^2 + 0.0000972 S^2 - 0.08735 L^2 \quad (3)$$

**Table 7**  
ANOVA analysis for Weld Area (WA)

Source	Sum of Squares	df	Mean Square	F Value	p-value Prob > F	
Model	507.6145	9	56.4016	103.9166	4.49827E-13	significant
I-Welding Current	302.8358	1	302.8360	557.9568	1.94121E-14	
S-Welding Speed	99.2523	1	99.2523	182.8663	1.58512E-10	
L-Arc Length	31.4205	1	31.4210	57.8904	7.17696E-07	
IS	57.6574	1	57.6574	106.2304	9.92404E-09	
IL	6.8685	1	6.8685	12.6549	0.0024	
SL	0.0055	1	0.0055	0.01026	0.9205	
I <sup>2</sup>	9.1740	1	9.1741	16.9027	0.0007	
S <sup>2</sup>	0.3543	1	0.3543	0.6529	0.4303	
L <sup>2</sup>	0.0457	1	0.0457	0.0843	0.7750	
Residual	9.2268	17	0.5428			
Cor Total	516.8414	26				

**Table 8**  
R-Squared value for Weld Area (WA)

Std. Dev.	0.7367	R-Squared	0.9821
Mean	4.4700	Adj R-Squared	0.9727
C.V. %	16.4813	Pred R-Squared	0.9484
PRESS	26.6854	Adeq Precision	34.8510

## 4. RESULTS AND DISCUSSION

As per the ANOVA experiment, the factors welding speed (S), welding current (I), and arc length (L) and interface factors such as IS, IL, SL and quadratic terms have significant impact on the Bead width (BW), Depth of penetration (DoP) and weld area(WA). The developed RSM models are utilized to find the impact of process variables and its interactions on the responses. Between any two process parameter the interaction effect is being analysed such as IS, SL, and IL, the center level will hold the third parameter.

### 4.1. Impact of input variables on Depth of Penetration (DoP)

The normal plot of residuals for DoP is shown in Fig. 5. The observed estimation and the predicted estimation of the responses are very close and it indicates almost exact the same for the developed model for DoP and it validates the same. From the contour plot between welding speed (S) and welding current (I) is shown in Fig. 6(a), the raise in welding current and slow in welding speed the DoP of the sheet increases. When the welding current (I) increases from 62 A to 79 A and welding speed (S) decreases from 350 to 250 mm/sec the DoP increases by 0.2 mm to 0.9 mm and percentage of DoP increased by 45 and nearly the half of the sheet thickness the DoP is attained. Then the welding current (I) increases from 80 A to 91 A and welding speed (S) decreases from 350 to 250 mm/sec and the DoP increases by 0.75 mm to 1 mm, more than 92 A to 100 A and the welding speed (S) increases from 250 to 310 mm/sec attains the 1.3 mm to 2 mm DoP and percentage of DoP increased by 45 and nearly the full of the sheet thickness the DoP is achieved. From the contour plot between welding current (I) and Arc Length (L) is depicted in Fig. 6(b), the raise in welding current (I) and low arc length (L) the DoP of the sheet increases. When the welding current (I) increases from 77 A to 91 A and arc length (L) decreases from 4 mm to 2 mm the DoP increases by 0.6 mm to 1.5 mm and percentage of DoP increased by 50 and nearly the two third of the sheet thickness the DoP is attained, more than 92 A to 100 A and arc length (L) 4 to 2 mm attains the 1.3 mm to 2 mm DoP and percentage of DoP increased by 40 and nearly the full of the sheet thickness the DoP is achieved. From the contour plot between welding speed (S) and Arc Length (L) is given in Fig. 6(c), the low arc length (L) and the decrease

in welding speed (S) DoP of the sheet increases. When the welding speed (S) reduced from 270 to 250 mm/sec and arc length (L) less than 2.2mm the DoP increases by 1.2 mm to 2 mm and percentage of DoP increased by 45 and nearly the full of the sheet thickness the DoP achieved.

From the 3D surface plot for interaction effects such as IS, IL and SL for DoP are displayed in Figs. 7(a)-(c), it is also evident that high welding current (I), low welding speed (S) and low arc length (L) results in a maximum DoP in AA-GTA welding process. From the ANOVA, it is very clear that welding current (I) has a high impact on the DoP (refer Table 3). The interaction effect between welding current (I) and welding speed (S) is displayed by the surface plot in Fig. 7(a), when the welding current (I) increases from 90 A to 100 A and welding speed (S) decreased from 350 to 250 mm/sec the DoP increases from 1 mm to 2 mm and percentage increase in DoP by 50, also attains the full penetration. For the interaction effect between welding current (I) and arc length (L) is displayed by the surface plot in Fig. 7(b), An increase in welding current and decrease in arc length from 3 mm to 2 mm causes an increase in DoP from 1mm to 2 mm. It also causes percentage increase in DoP by 45, attaining the full depth of penetration. For the interaction effect between welding speed (S) and arc length (L) is displayed by the surface plot in Fig. 7(c), An increase in welding speed and decrease in arc length from 3 mm to 2 mm causes an increase in DoP from 1mm to 2 mm. It also causes percentage increase in DoP by 50, attaining the full depth of penetration.

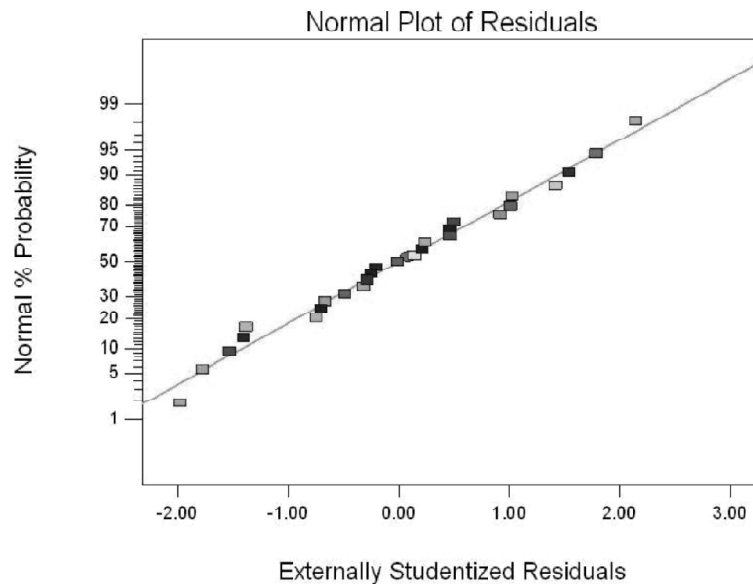


Figure 5: Normal plot of Residuals for Depth of Penetration (DoP)

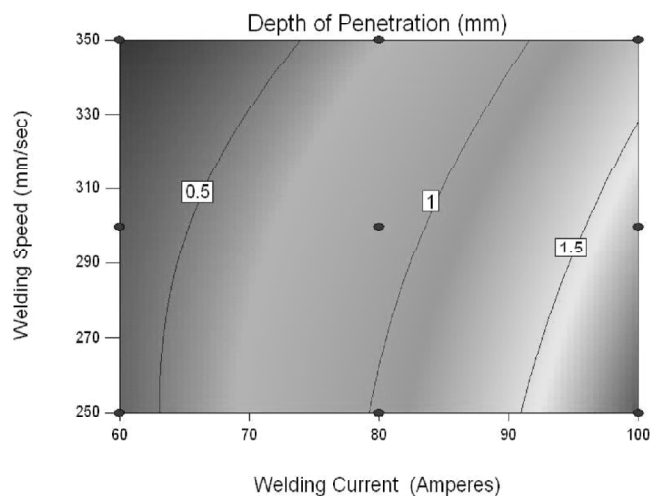


Figure 6(a): Contour plot Welding current(I) Vs Welding Speed (S) for Depth of Penetration (DoP)

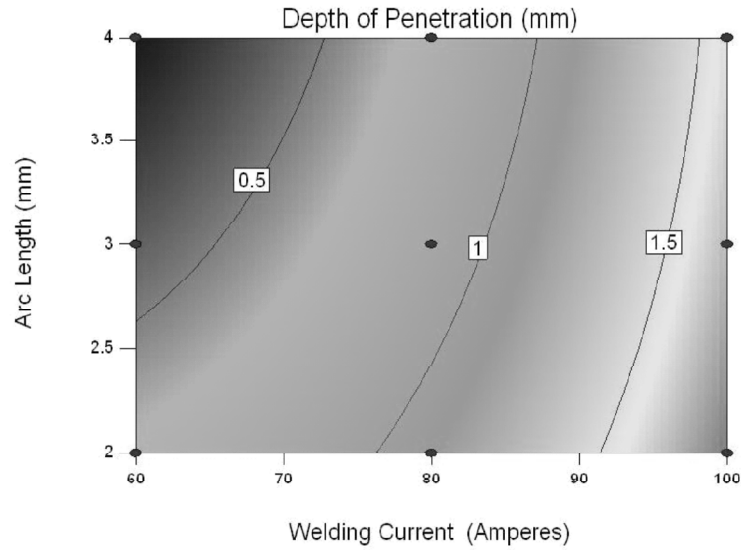


Figure 6(b): Contour plot Welding current (I) Vs Arc Length (L) for Depth of Penetration (DoP)

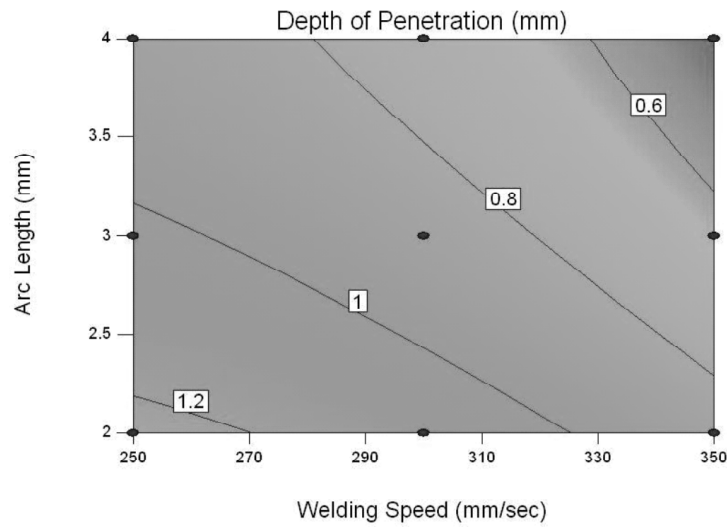


Figure 6(c): Contour plot Welding speed (S) Vs Arc Length(L) for Depth of Penetration (DoP)

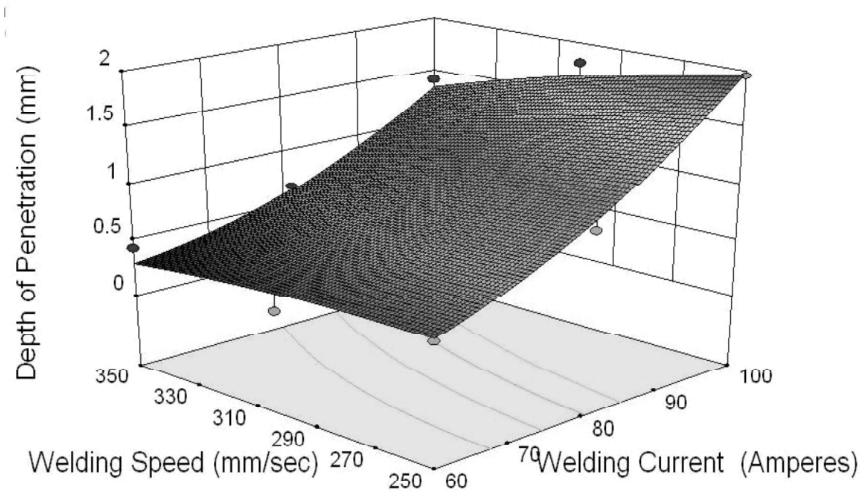


Figure 7(a): 3D surface plot for interaction effect of IS on Depth of Penetration (DoP)

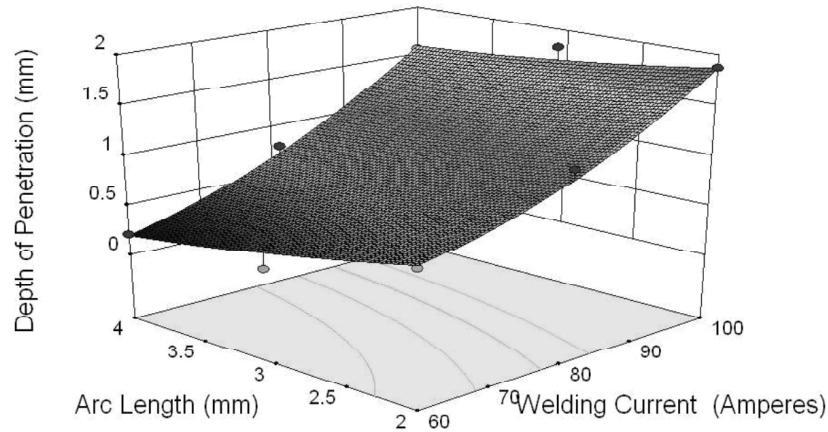


Figure 7(b): 3D surface plot for interaction effect of IL on Depth of Penetration (DoP)

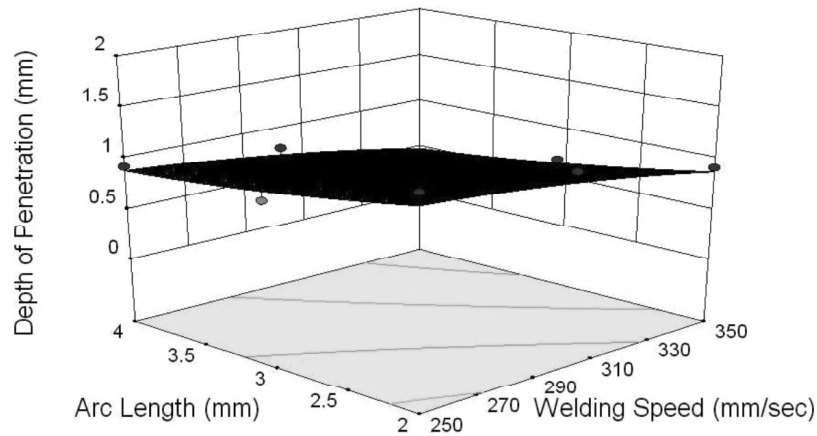


Figure 7(c): 3D surface plot for interaction effect of SL on Depth of Penetration (DoP)

#### 4.2. Effect of input variables on Bead Width (BW)

The normal plot of residuals for BW is shown in Fig. 8. The noted estimation and the expected estimation of the responses are very close and it indicates exact the same for the improved model for BW and it validates the same. From the contour plot between welding speed (S) and welding current (I) is displayed in Fig. 9(a), the decrease in welding current (I) and increase in welding speed (S) the BW of the sheet decreases. When the welding current (I) decreases from 100 A to 93 A and welding speed (S) increases from 250 to 350 mm/sec the BW decreases by 14.8 mm to 6 mm and percentage of BW decreased by 50 and nearly the half of the BW decreased. Then the welding current (I) decreases from 90 A to 70 A and welding speed (S) increases from 250 to 350 mm/sec and the BW decreases by 4.2 mm to 2.2 mm percentage of BW decreased nearly 10, less than 70 A attains the BW less than 2 mm. From the contour plot between welding current (I) and Arc Length (L) is displayed in Fig. 9(b), the low arc length (L) and decrease in welding current (I) the BW of the sheet decreases. When the welding current (I) decreases from 100 A to 93 A and arc length (L) decreased from 4 to 2 mm the BW decreases by 14.8 mm to 5 mm and percentage of BW decreased by 65 and nearly the two third of the BW decreased. The welding current (I) decreases from 92 A to 70 A and arc length (L) 4 to 2 mm attains the 5.5 mm to 2.3 mm BW and percentage of BW decreased by 20. From the contour plot between arc length (L) and welding speed (S) is displayed in Fig. 9(c), the increase in welding speed (S) and low arc length (L) the BW of the weld decreases. When the welding speed (S) increased from 270 to 310 mm/sec and arc length (L) decreases from 4 to 2 mm, the BW decreases by 5 mm to 3.2 mm.

From the 3D surface plot for interaction effects such as IS, IL and SL for BW are shown in Figs. 10(a)-(c), it is also evident that high welding speed (S), low welding current (I), and low arc length (L) results in a minimum BW in AA-GTA welding process. From the ANOVA analysis it is also revealed that welding current (I) has a huge impact on the BW (refer Table 5). The interaction effect between welding speed (S) and welding current (I) is shown as surface plot in Fig. 10(a), when the welding current (I) decreases from 90 A to 80 A and welding speed (S) increased from 250 to 350 mm/sec the BW decreases from 5.5 mm to 3 mm and percentage decreases in BW by 15. The interaction effect between welding current (I) and arc length is shown as surface plot in Fig. 10(b), when the welding current (I) decreases from 90 A to 70 A and arc length decreased (L) from 3.5 to 2.5 mm the BW decreases from 5 mm to 2.5mm. The interaction effect between welding speed (S) and arc length (L) is shown as surface plot in Fig. 10(c), when the welding speed (I) decreases from 350mm/sec to 250mm/sec and arc length decreased (L) from 3.5 to 2.5 mm the BW decreases from 4.5 mm to 3 mm.

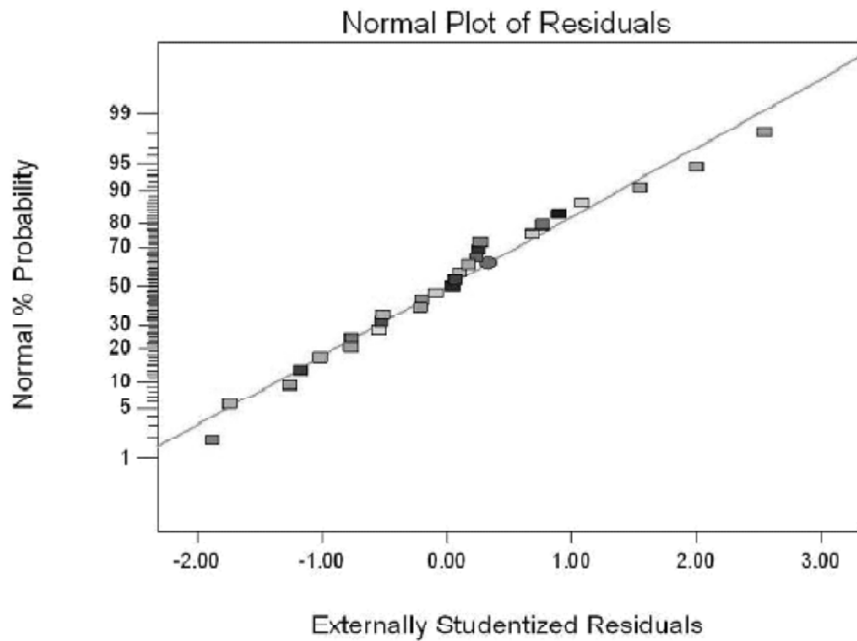


Figure 8: Normal plot of Residuals for Bead Width (BW)

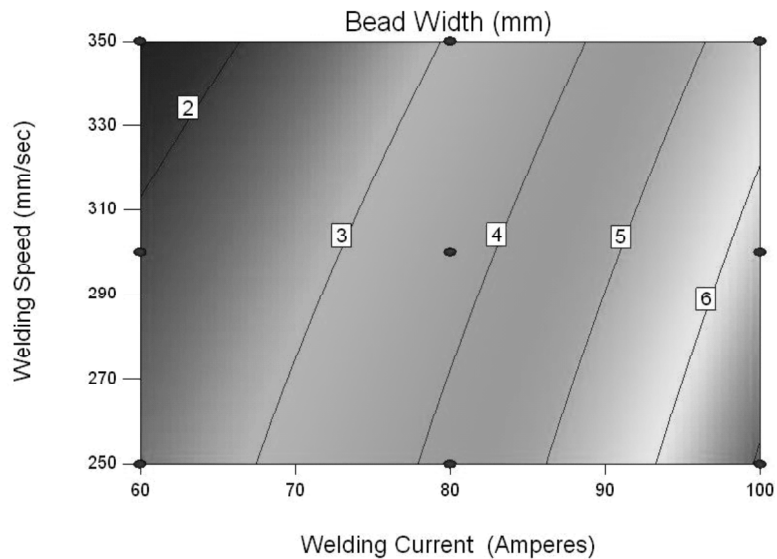


Figure 9(a): Contour plot Welding current (I) Vs Welding Speed (S)for Bead Width (BW)

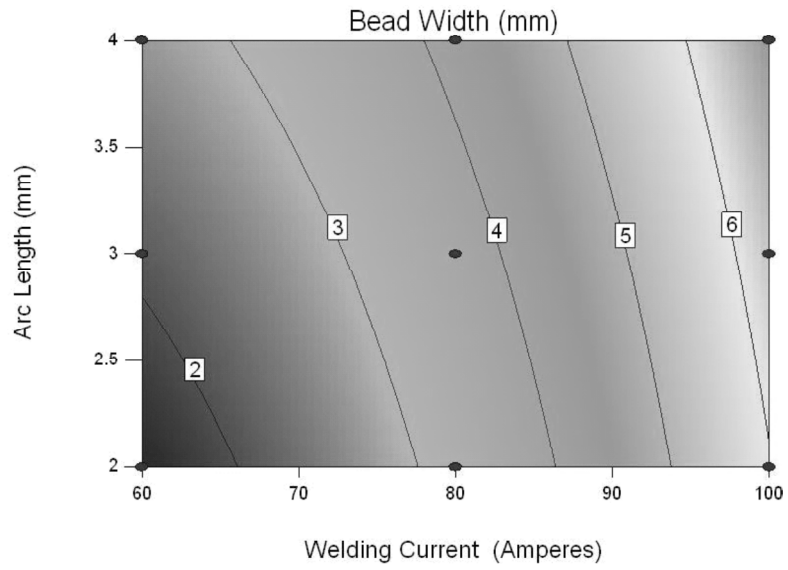


Figure 9(b): Contour plot Welding current (I) Vs Arc Length(L) for Bead Width (BW)

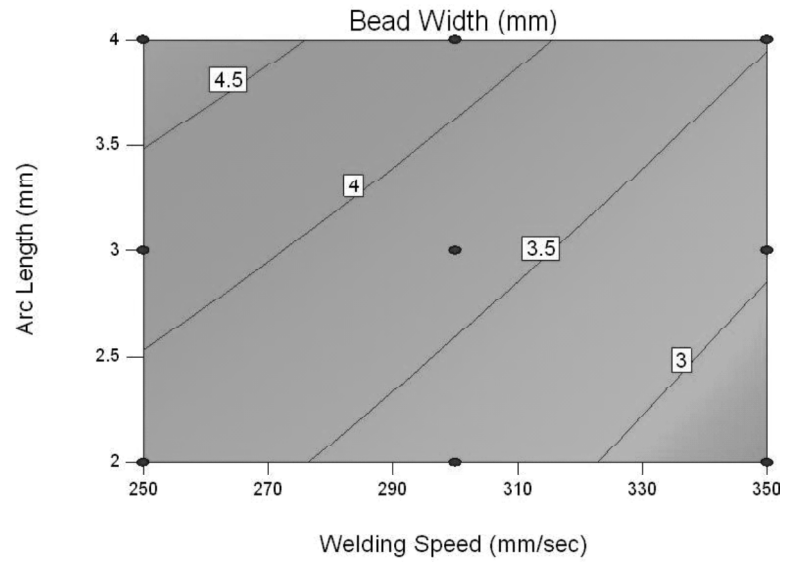


Figure 9(c): Contour plot Welding speed (S) Vs Arc length(L) for Bead Width (BW)

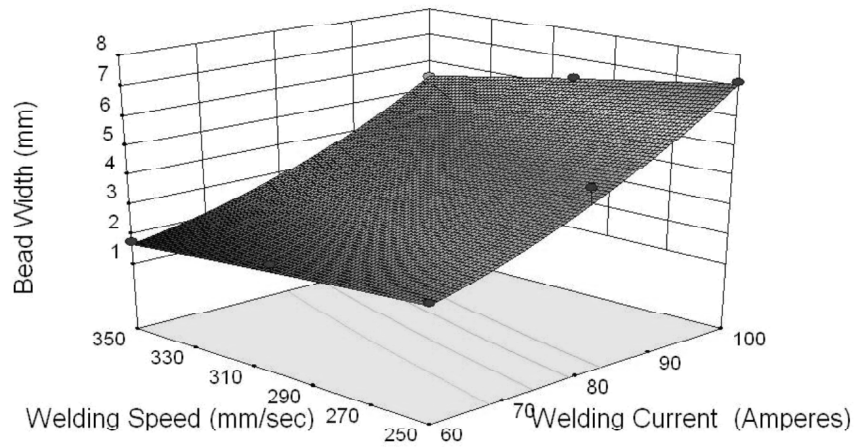


Figure 10(a): 3D surface plot for interaction effect of IS on Bead Width (BW)

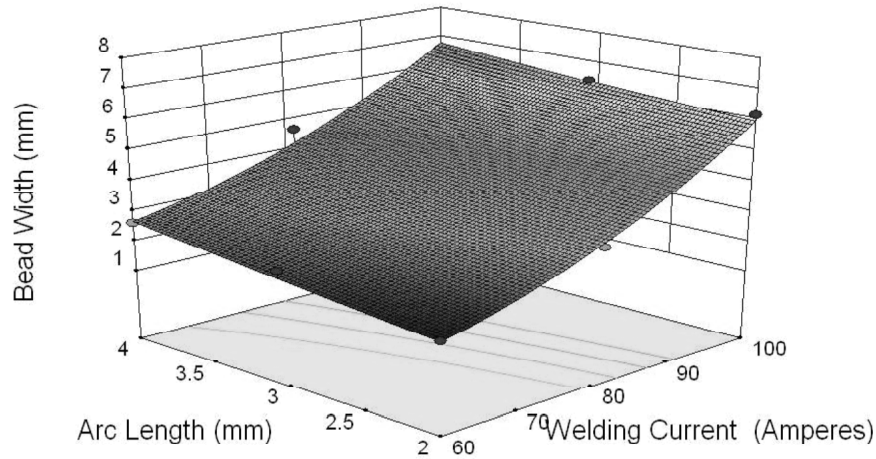


Figure 10(b): 3D surface plot for interaction effect of IL on Bead Width (BW)

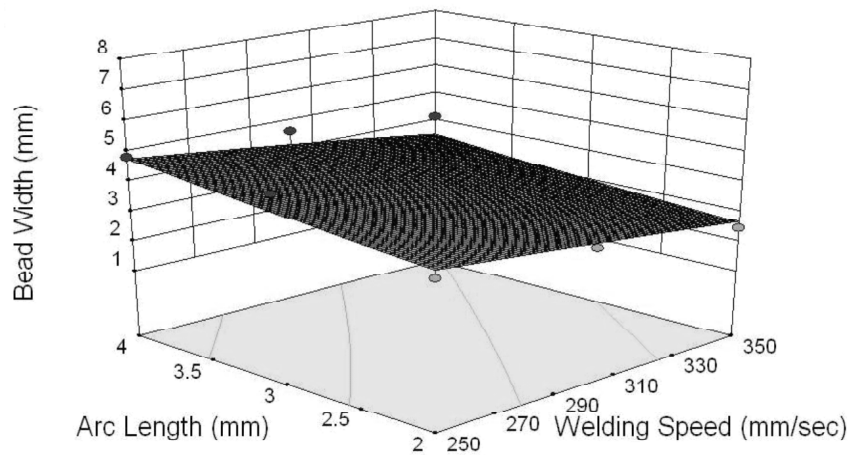


Figure 10(c): 3D surface plot for interaction effect of SL on Bead Width (BW)

#### 4.3. Effect of input variables on Weld Area (WA)

The normal plot of residuals for Weld area is displayed in Fig. 11. The noted estimation and the expected estimation of the responses are very close and it indicates exact the same for the developed model for WA and it validates the same. From the contour plot between welding speed (S) and welding current (I) is shown in Fig. 12(a), the increase in welding current (I) and slow speed (S) the WA of the sheet increases. When the welding current (I) increases from 64 A to 80 A and welding speed (S) decreases from 350 to 250 mm/sec the WA increases by 1.5 mm to 6 mm and percentage of WA increased by 30 and nearly the one third of the WA attained. Then the welding current (I) increases from 81 A to 91 A and welding speed (S) decreases from 350 to 250 mm/sec and the WA increases by 2 mm to 10 mm, more than 92 A to 100 A and the welding speed (S) 350 to 250 mm/sec attains the 3.8 mm to 14.8 mm WA and percentage of WA increased by 70. From the contour plot between welding current (I) and Arc Length (L) is displayed in Fig. 12(b), the increase in welding current (I) and low arc length (L) the WA of the sheet increases. When the welding current (I) increases from 70 A to 91 A and arc length (L) decreases from 4 mm to 2 mm the WA increases by 1.8 mm to 8 mm and percentage of WA increased by 50, more than 92 A to 100 A and arc length (L) 4 to 2 mm attains the 8 mm to 14.8 mm WA and percentage of WA increased by 40 and nearly the maximum WA is achieved. From the contour plot between welding speed (S) and Arc Length (L) is shown in Fig. 12(c), the decrease in welding speed (S) and low arc length (L) the WA of the sheet increases. When

the welding speed (S) reduced from 310 to 270 mm/sec and arc length (L) 4 to 2 mm the WA increases by 1.9 mm to 6.2 mm and percentage of WA increased by 35.

From the 3D surface plot for interaction effects such as IS, IL and SL on WA are shown in Fig. 13(a)-(c), it is also evident that high welding current (I), low welding speed (S) and low arc length (L) results in a maximum WA in AA-GTA welding process. From the ANOVA, it is further evident that welding current has a large impact on the WA (refer Table 7). The interaction effect between welding current (I) and welding speed (S) is given as surface plot in Fig. 13(a), when the welding current (I) increases from 90 A to 100 A and welding speed (S) decreased from 350 to 250 mm/sec the WA increases from 3 mm to 14.8 mm and percentage increase in WA by 80, also attains the maximum WA. The interaction effect between welding current (I) and arc length (L) is shown as surface plot in Fig. 13(b), when the welding current starts from 80 A to 100 A and arc length decreased from 3 to 2mm the WA increases from 3.5 mm to 14.8 mm and percentage increase in WA by 80, also attains the maximum WA. The interaction effect between welding speed (I) and arc length (L) is shown as surface plot in Fig. 13(c), when the welding speed decreases from 350mm/sec to 250mm/sec and arc length decreased from 4 to 2mm the WA increases from 3 mm to 14.8 mm and percentage increase in WA by 80, also attains the maximum WA.

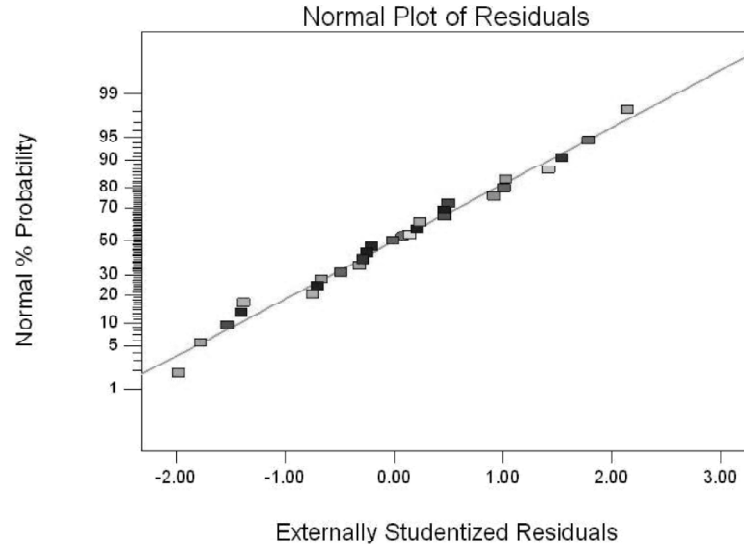


Figure 11: Residual plot for Weld area (WA)

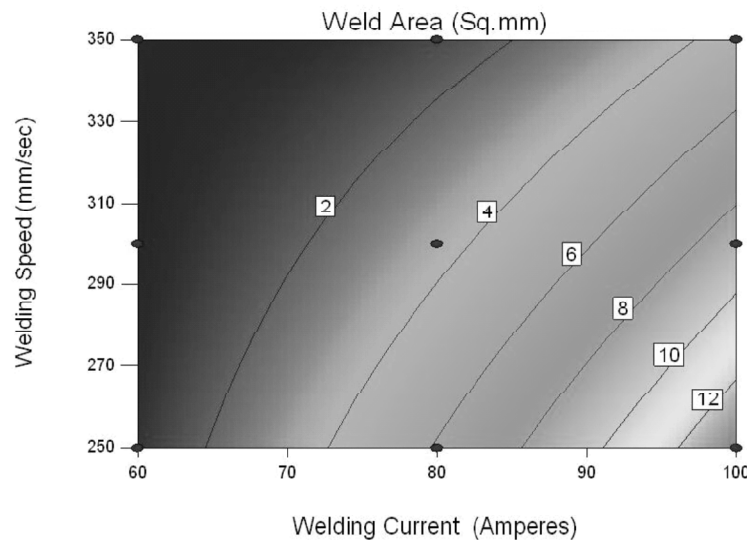


Figure 12(a): Contour plot Welding current (I) Vs Welding Speed (S) for Weld Area (WA)

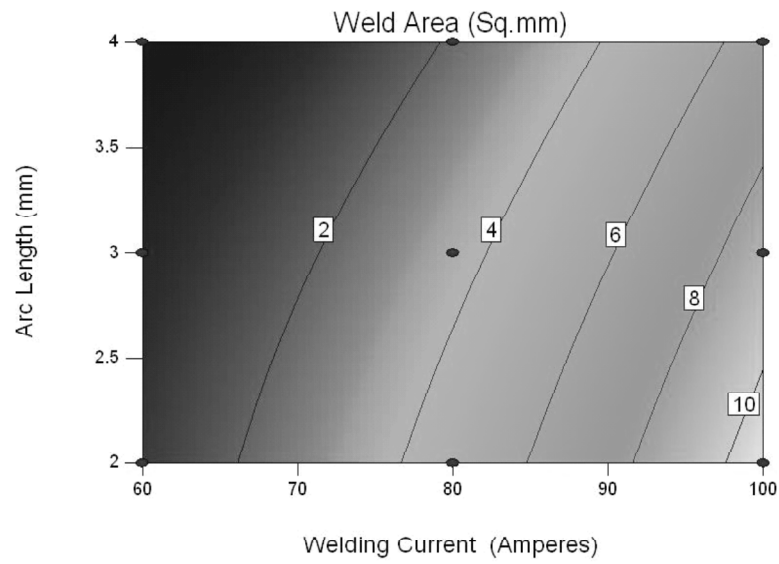


Figure 12(b): Contour plot Welding current (I) Vs Arc length (L) for Weld Area (WA)

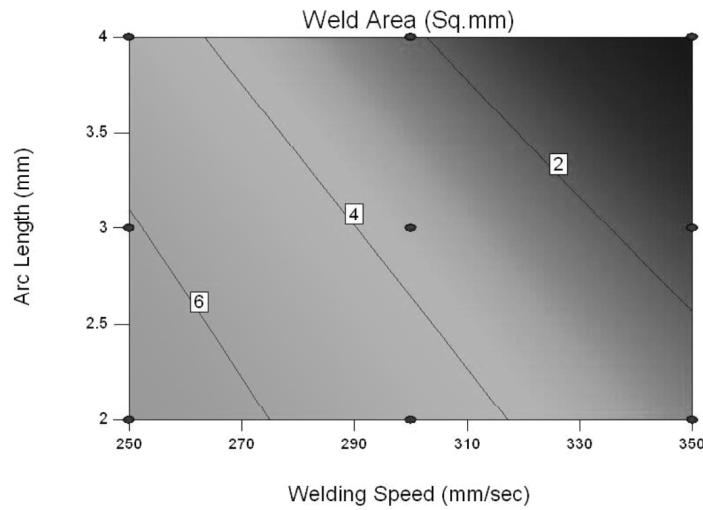


Figure 12(c): Contour plot Welding speed (S) Vs Arc length (L) for Weld Area (WA)

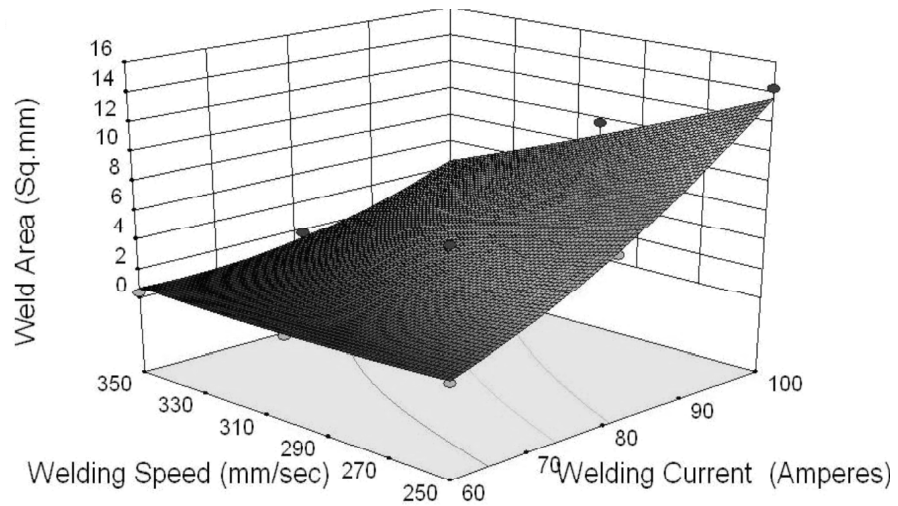


Figure 13(a): 3D surface plot for interaction effect of IS on Weld Area (WA)

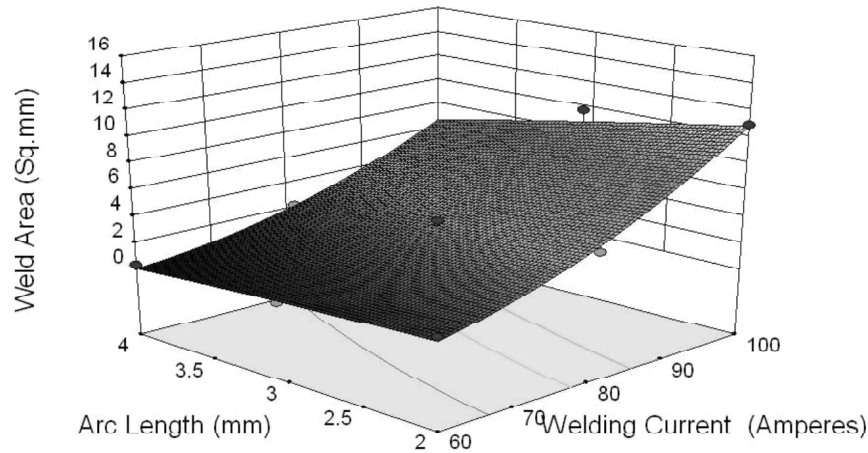


Figure 13(b): 3D surface plot for interaction effect of IL on Weld Area (WA)

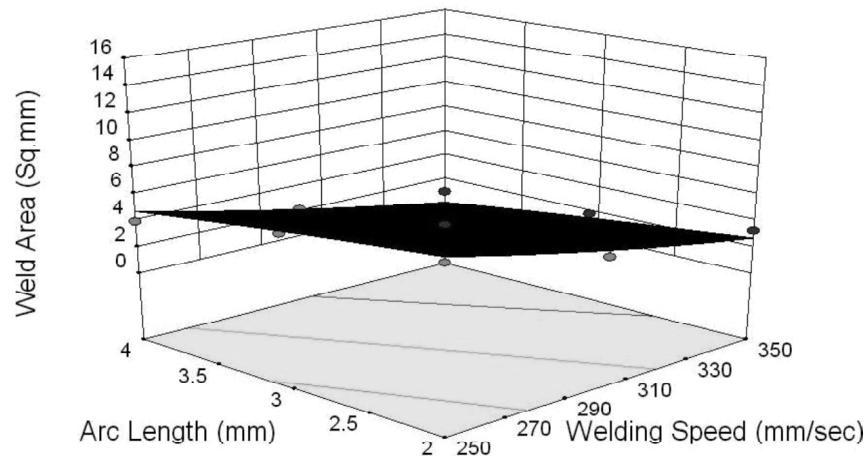


Figure 13(c): 3D surface plot for interaction effect of SL on Weld Area (WA)

## 5. OPTIMIZATION OF INPUT VARIABLES

Input variables optimization searches fusion of factor levels and that which satisfy the criteria on each step of the responses and input variables. Numerical optimization technique combines the goals in to an overall desirability function (D). In AA-TIG welding process of 2205 DSS, the aim is to maximize the Depth of penetration, weld area and minimize the bead width for the given process parameters range. The input process parameters ranges are set in as presented in Table 2. Then calculate the desirability and it is 0.963. The desirability of the design meets the standard value. According to desirability the optimum weld bead geometry conditions as per the criteria that would result in maximum Depth of Penetration (DoP) is about 2.0601 mm, minimum Bead Width (BW) is about 6.8129mm and maximum weld area (WA) is about 14.8731mm<sup>2</sup>. These are achieved by the input variables such as welding current (I) 100 A, Welding speed (S) 250 mm/sec and arc length (L) 2.4 mm.

## 6. VALIDATION

Table 9 furnishes a set of optimal solution, parameter for welding current (I) has to be 100Amperes and welding speed (S) has to be 250 mm/sec and arc length (L) has to be 2.4 mm. The combination of process parameters with highest desirability value is chosen which functions as the optimized geometry of weld bead conditions. The validation experiment is conducted to obtain optimal solution which is evident in the model. The input parameter set is chosen from optimal solution for validation experiment. To calculate the

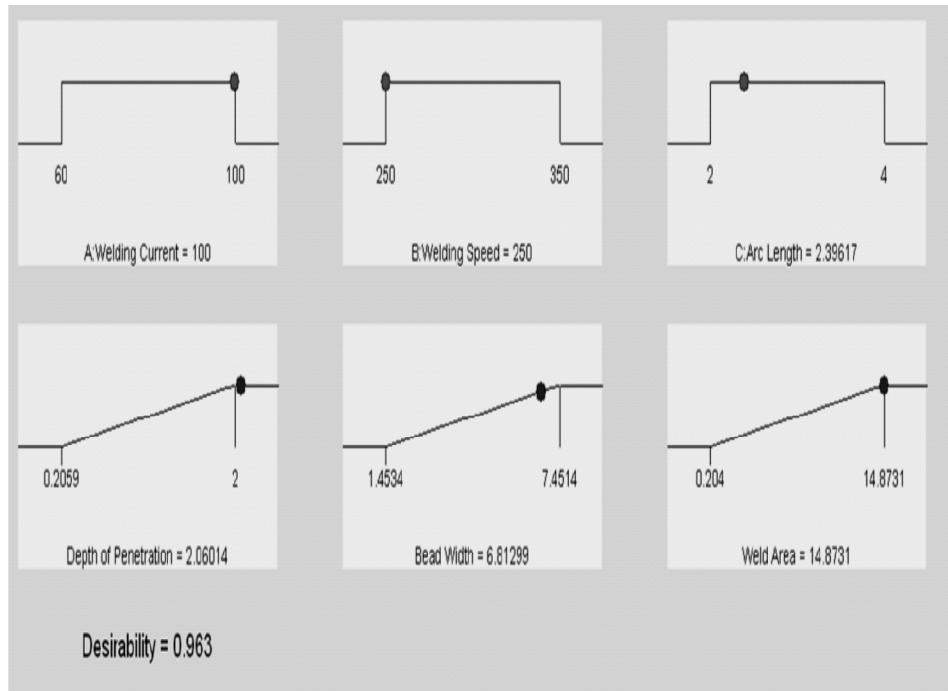


Figure 14: Ramp diagram with optimized input parameter and predicted responses

error, the actual value and the model predicted value is indicated for the validation set as displayed in Table 9. For computation of Percentage Error is the ratio of difference between actual value and predicted value to the predicted value. There was a very less percentage of error and the value less than 4%, which shows the model fairly accurate.

Table 9  
Validation of test results

<b>Depth of Penetration</b>	Actual Value	1.9802
	Predicted Value	2.0601
	% of Error	1.9417
<b>Bead Width</b>	Actual Value	6.5230
	Predicted Value	6.8129
	% of Error	4.2564
<b>Weld Area</b>	Actual Value	14.3595
	Predicted Value	14.8731
	% of Error	3.4532

## 7. CONCLUSIONS

In this paper, a report is made on the selection of the input variables for the autogenous automated GTA welding of 2205 DSS with optimal weld pool geometry. The following are the conclusions that are drawn during the present investigation:

- For process parameters optimization and for AA-GTA welding of 2205 DSS, RSM is found to be an accurate method. The responses of Bead Width (BW), Depth of penetration (DOP), and Weld area (WA) are predicted by applying second order quadratic model.
- The optimum input variables such as Welding current (I)- 100A, welding speed (S) 250mm/sec and arc length (L) 2.4mm are set to achieve the preferred responses of weld bead geometry which

consists of maximum Depth of Penetration (DoP) of approximately 2.0601 mm, minimum Bead width (BW) of about 6.8129 mm and maximum weld area (WA) of about 14.8731 mm<sup>2</sup>.

- As per the ANOVA analysis the interaction effect of welding current–welding speed (IS) is most significant when compared to other interaction effect of welding current–arc length (IL) and arc length–welding speed (LS) are less significant. For high welding current (I), low welding speed (S) and low arc length (L) maximum Depth of penetration (DoP) and weld area (WA) are occurred. For high welding current (I), high arc length (L) and low welding speed (S) minimum Bead Width (BW) was obtained.
- From the optimized set of input variables such as welding current (I)- 100A, welding speed 250 mm/sec and arc length (L) 2.4mm, the experiments were conducted and the experimental responses obtained include a maximum Depth of Penetration of about 1.9802 mm, minimum Bead Width of about 6.5230mm and maximum weld area A of about 14.3595 mm<sup>2</sup>. The error percentage is very minimum and it is less than 5% and the model is fairly accurate.

## REFERENCES

- [1] H. Farnoush, A. Momeni, K. Dehghani, J. Aghazadeh Mohandesi and H. Keshmiri, "Hot deformation characteristics of 2205 duplex stainless steel based on the behavior of constituent phases", *Materials & Design*, Vol. 31, Issue 1, 2010, pp. 220–226.
- [2] K. Yurtisik, Suha Tirkes, I. Dykhno, C.H. Gur and R. Gurbuz, "Characterization of duplex stainless steel weld metals obtained by hybrid plasma-gas metal arc welding", *Soldagem & Inspeção*, Vol. 18 No. 3, 2013, pp. 207-216.
- [3] R.S. Parmar, "Welding engineering and technology", Second Edition, 2013, Khanna Publishers, New Delhi.
- [4] B. Bonnefois, R. Blondeau and D. Catelin, "Control of the Ferrite Level in Duplex Stainless Steel Welds," *Proceedings of International Conference, Duplex Stainless Steel*, The Hague, 27-28 October 1986, paper 6.
- [5] Y.S Tarnq, H.L Tsai and S.S Yeh, "Modeling, optimization and classification of weld quality in tungsten inert gas welding", *International Journal of Machine Tools and Manufacture*, Vol. 39 No. 9, 1999, pp. 1427-1438.
- [6] X.L. Gao, L. Zhang, J. Liu and J.X. Zhang, "A comparative study of pulsed Nd:YAG laser welding and TIG welding of thin Ti6Al4V titanium alloy plate", *Materials Science and Engineering A* Vol. 559, 2013, pp. 14–21
- [7] C. Meran, "Prediction of the optimized welding parameters for the joined brass plates using genetic algorithm", *Materials & Design*, Vol. 27, Issue 5, 2006, pp. 356–363.
- [8] G. Magudeeswaran, S.R. Nair, L. Sundar and N. Harikannan, "Optimization of process parameters of the activated tungsten inert gas welding for aspect ratio of UNS S32205 duplex stainless steel welds", *Defence Technology*, Vol. 10, Issue 3, 2014, pp. 251–260.
- [9] N. Kiaee and M.A. Khafri, "Optimization of gas tungsten arc welding process by response surface methodology", *Materials & Design*, Vol. 54, 2014, pp. 25–31.
- [10] S.C Juang and Y.S Tarnq, "Process parameter selection for optimizing the weld pool geometry in the tungsten inert gas welding of stainless steel", *Journal of Materials Processing Technology*, Volume 122, Issue 1, 2002, pp. 33–37.
- [11] A. Karpagaraj, N. Siva Shanmugam and K. Sankaranarayanan, "Some studies on mechanical properties and microstructural characterization of automated TIG welding of thin commercially pure titanium sheets", *Materials Science and Engineering: A*, Vol. 640, 2015, pp. 180–189.
- [12] N.N. Korra, M. Vasudevan and K. R. Balasubramanian, "Multi-objective optimization of activated tungsten inert gas welding of duplex stainless steel using response surface methodology", *The International Journal of Advanced Manufacturing Technology*, Vol. 77, Issue 1, 2015, pp. 67–81
- [13] K.Y. Benyounis and A.G. Olabi, "Optimization of different welding processes using statistical and numerical approaches – A reference guide", *Advances in Engineering Software*, Vol. 39, Issue 6, 2008, pp. 483–496.
- [14] H.M. Ibrahim and E.E. Elkhidir, "Response Surface Method as an Efficient Tool for Medium Optimisation", *Trends in Applied Sciences Research*, Vol. 6, pp. 121-129.
- [15] R. Kadaganchi, M.R. Gankidi and Hina Gokhale, "Optimization of process parameters of aluminum alloy AA 2014-T6 friction stir welds by response surface methodology", *Defence Technology*, Vol. 11, Issue 3, 2015, pp. 209–219.